

Spotweld Modeling Methodologies and Failure Characterization of Aluminum Resistance Spotwelds (RSW) using LS-DYNA

Akshay Kulkarni ¹, Ashwin Yeagappan ¹, Joao Moraes ¹, Lily Slabbert ¹, Martin Vézina ²

¹Novelis Customer Solution Center, Novi, MI (USA)

²Thumbprint Solutions Inc., ON (Canada)

Abstract

With an increased use of aluminum in automotive body structures, developing a deep understanding, and capability to model failure of aluminum resistance spotwelds (RSWs) is critical [1]. This paper discusses failure card development of aluminum RSWs using LS-DYNA for certain 5000 and 6000 series flat rolled sheet alloys used in automotive structural applications.

A detailed study and comparison of various material models was conducted, and an appropriate model was chosen to effectively achieve the project objectives. Several CAE sensitivity studies of failure parameters, weld modeling techniques, weld element orientation, parent material mesh size were conducted. Findings helped to select the preferred modeling approach.

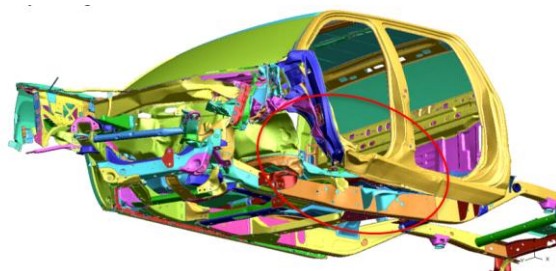
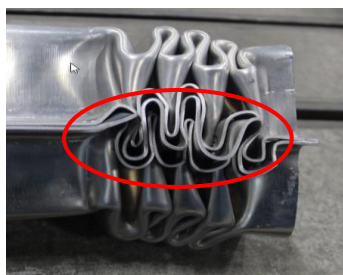
Various methods in failure model to improve axial loading prediction were evaluated and compared. Numerous simulations were run to study 'post-failure damage' modeling using *MAT_100_DA model. Results indicated what care should be taken while using damage and using hex clusters. This paper examines the efficacy of different testing methods including flat coupon testing (Lap shear, Cross tension, and Coach peel) and KS-2 testing. The paper also documents the types of tests conducted to develop the failure cards and shows test to CAE correlation.

Overall, this paper delves into the failure modelling possibilities of resistance spot welding for aluminum sheets, investigating the impact of each variable involved in the modelling process. It also compares CAE results with physical test data and gives recommendations on preferred modeling approach.

1 Introduction

Latest industry trends show that use of aluminum sheet, extrusions and large castings is increasing in vehicle bodies as well as battery enclosures. Aluminum is becoming a material of choice to achieve lightweighting and sustainability benefits [2] [3]. This work discusses failure card development of aluminum RSWs using LS-DYNA for certain 5000 and 6000 series alloys used in structural applications.

Robust joints in automotive body structure play vital role in structural performance during crash events [4]. Having an in depth understanding of failure behavior of RSWs is critical and helps automotive original equipment manufacturers (OEMs) design aluminum intensive structures to meet important safety regulations. Realistic spotweld failure definitions in CAE models help predict weld failure in various crash modes which eventually reduces the number of test prototypes. Two examples of weld failure have been shown in Fig.1. Image on left hand side shows failed welds in axial crush while image on the right is from IIHS small offset rigid barrier impact of a public domain CAE model of a pickup truck.



Public Domain CAE Model Source: <https://www.nhtsa.gov>

Fig. 1: Weld failure in component and full vehicle level

The objective of this project was to characterize the weld failure of aluminum RSWs for certain 5000 and 6000 series aluminum sheet alloys. While calibrating failure cards, the primary goal was to match total energy absorbed while minimizing deviation from the failure stress measured from weld coupon tests.

LS-DYNA offers multiple options of defining spotweld elements and their failure properties. An appropriate method can be chosen based on the required level of accuracy, consistency in results, modeling convenience and reverse engineering effort. The term 'reverse engineering' in this paper is the process where failure parameters in FEA model are adjusted to match test curves irrespective of deviation from the test data. Spotweld can be modeled using beam elements, solid elements, solid hex assemblies or using ***CONSTRAINED** keywords like ***CONSTRAINED_SPOTWELD**, ***CONSTRAINED_INTERPOLATION_SPOTWELD** (Fig. 2).



Fig.2: Different types of weld representation in LS-Dyna

Multiple material models are available in LS-DYNA which can be used to define failure properties of RSWs [5],[6]. A detailed comparison study was conducted, and an appropriate material model was selected to achieve the objectives of the project. Details are discussed in the next section. ***MAT_100_DA** was selected for failure card calibration in this project for the reasons elaborated in the next section. Several CAE sensitivity studies were conducted to understand the effect of failure parameters on weld failure prediction. DOE study for ***MAT_100_DA** key failure parameters (SIGY, ETAN, SB, SN, SS, EX) was conducted to understand contribution of each in various stress states (0°, 30°, 60°, 90° loading angles and Peel). DOE study of weld element modeling techniques, weld element orientation, parent material mesh size was conducted. Data generated from these sensitivity studies resulted in interesting insights which helped in recommending preferred modelling approach for this activity.

This paper elaborates on post-failure damage modeling options available while using 0. For instance, it was found that the UNIAXIAL option does not fulfill its promises when the plates joined have different stiffness and a hex cluster is used (with ***DEFINE_SPOTWELD_ASSEMBLY**). The hex cluster must be in a uniaxial stress state for the damage function to grow as expected. Two plates with different stiffness put certain elements of hex cluster in a mixed stress state i.e., a mix of shear and tension. Local deformation in the plates generates shear stress components in hex cluster if stiffness is different. The behavior during damage depends on how fast the hex cluster will reach (or not reach at all) a uniaxial tension stress state.

Rigorous weld development and physical testing activities were involved during this project. Process followed to develop good quality welds and various types of coupon tests have been discussed in this paper. Coupon tests included flat coupon tests and KS-2 specimen tests. Process of developing failure parameters and CAE-test correlation examples have been elaborated.

2 Weld Failure Material Models in LS-DYNA

Many material models exist in LS-DYNA for modelling failure of RSW joints. Each material model has its own advantages and limitations related to the governing equation of the failure calculation, number of inputs, reverse engineering effort, post-failure damage behavior accuracy, and types of elements supported. Key material models were studied in detail and have been summarized in this section.

MAT_100** (MAT_SPOTWELD**) model is a bilinear elastoplastic model which uses elastic plastic von mises formulation. This model ignores the damage function, thereby the weld element fails when the failure criteria are met. This is a force and moment-based failure model. Option **DAMAGE_FAILURE** enables additional features like invoking post-failure (damage) behavior, changing failure options through parameter **OPT**.

***MAT_100_DA (*MAT_SPOTWELD_DAIMLERCHRYSLER)** is a bilinear elastoplastic model, which works on a stress-based model [7]. This material model requires definition of ***DEFINE_CONNECTION_PROPERTIES** keyword where the failure and damage parameters of the weld are defined. This model provides more flexibility over the stress based ***MAT_SPOTWELD_DAMAGE_FAILURE** (OPT=6) by having separate bending and axial terms. Exponents on failure terms (EXSN, EXSB, EXSS) provide more flexibility to tune the final set of parameters and improve correlation. Post-failure damage can be defined through choosing the desired DGTYP option.

***MAT_COHESIVE_MIXED_MODE_ELASTOPLASTIC_RATE (*MAT_240)** is a rate dependent, Trilinear elastic ideally plastic model. This model is used for cohesive elements and the damage initiation is governed by a power law. MAT_240 is a stress-based model developed for modelling adhesives. This model uses yield strengths in tangential and shear directions and defined using energy-related parameters. These models require many parameters requiring high reverse engineering effort.

***CONSTRAINED_INTERPOLATION_SPOTWELD** is an advanced model of ***CONSTRAINED_SPR_2** which was initially developed for self-piercing rivets (SPR) but can be used for spotwelds too. The forces and moments are calculated based on the relative movements of the connected sheets. This is a plasticity-based damage model. The resultant forces and moments are ramped down to zero once the failure criterion is met, resulting in a linear damage curve. This model provides better failure prediction compared to other models; however, it is a complex model requiring a greater reverse engineering effort for calibration. A limitation of this model is that it cannot be used for traditional 1D beam and 3D hex elements. Currently 3D hex elements and hex clusters are widely used in the automotive industry.

Table 1 summarizes comparison of all material models under study.

Material Model	Failure Function	Element Types Supported	Post Failure Damage	Remarks
*MAT_100	Force based	<ul style="list-style-type: none"> • Beam • Hex • Hex cluster 	No	<ul style="list-style-type: none"> • Very basic spotweld failure model • Gives rough approximation of failure behavior. • Constant exponent in the failure function limits the flexibility in card calibration. • Damage behavior is not captured
*MAT_100_DAMAGE_FAILURE	Force based/ Stress based	<ul style="list-style-type: none"> • Beam • Hex • Hex cluster 	Yes	<ul style="list-style-type: none"> • Simple spotweld failure model with post-failure damage. • Bending failure cannot be separately specified with stress-based failure. • Constant exponent in the failure function limits the flexibility in card calibration. • Issues in damage behavior for axial loading conditions with hex clusters.
*MAT_100_DA	Stress based	<ul style="list-style-type: none"> • Hex • Hex cluster 	Yes	<ul style="list-style-type: none"> • Bending failure can be defined separately. • Exponents provide flexibility to tune failure individually for axial, shear and bending. • Does not support beam elements. • Flexibility in defining damage by multiple approaches (DGTYP) • Issues in damage behavior for axial loading conditions with hex clusters. • Accuracy in axial loading and bending is limited.
*MAT_240	Stress based	<ul style="list-style-type: none"> • Hex • Hex cluster 	Yes	<ul style="list-style-type: none"> • Good accuracy in weld failure prediction. • Only works for cohesive elements. • More popular for adhesives.

				<ul style="list-style-type: none"> Reverse engineering the energy release rates might require considerable effort. Finding yield stress for two modes might be difficult.
*CONSTRAINED_INTERPOLATION_SPOTWELD	Force based	<ul style="list-style-type: none"> Weld is defined as an interpolation constraint 	Yes	<ul style="list-style-type: none"> Good accuracy in weld failure prediction. Higher reverse engineering effort is required to calibrate numerous parameters like exponents, scale factors, plastic initiation Displacement, rupture displacement etc. Modelling the SPR4 elements is tricky and difficult to automate at this point.
*MAT_24 with *MAT_ADD_DAMAGE_GISSMO	Triaxiality based	<ul style="list-style-type: none"> Hex Hex cluster 	Yes	<ul style="list-style-type: none"> Developing GISSMO cards for each stack would be a huge effort. Significant reverse engineering would be needed for defining triaxiality curve.

Table 1: Comparison Table showing various weld failure material models.

2.1 Material Model Used for Failure Characterization

***MAT_100_DA** model was chosen for this study based on:

- Reduced reverse engineering effort needed to give reasonable failure prediction.
- Flexibility to define separate bending failure.
- Flexibility to tune failure and improve correlation through exponents.
- Multiple options to define post-failure damage.

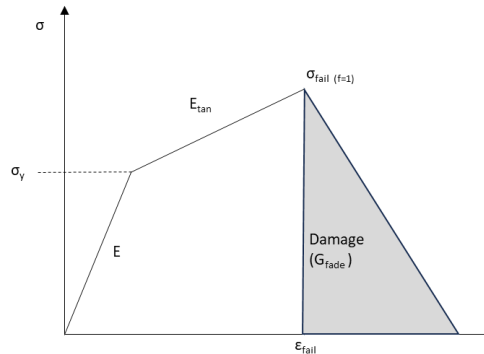


Fig.3: ***MAT_100_DA** Material Model Behavior

The failure function for this material model is defined by a three-parameter failure function governed by a power law (Eq.1). The damage behavior (Fig.3) provides more flexibility in choosing between strain-based, function based and fading energy-based damage. The damage initiates once the failure load is reached and represented by a linear softening curve. The slope of this curve is driven by input parameters Rupture Strain (RS) or GFAD depending on the type of damage. [8]

$$f = \left(\frac{\sigma_n}{SN}\right)^{D_EXSN} + \left(\frac{\sigma_b}{SB}\right)^{D_EXSB} + \left(\frac{\tau}{SS}\right)^{D_EXSS} \leq 1 \quad (1)$$

Where σ_n, σ_b, τ are normal, bending and shear stresses respectively. SN, SB, SS are normal, bending and shear failure stresses and D_EXSN, D_EXSB, D_EXSS are exponents. Fig.4 shows LS-DYNA keyword for ***MAT_100_DA** and ***DEFINE_CONNECTION_PROPERTIES**

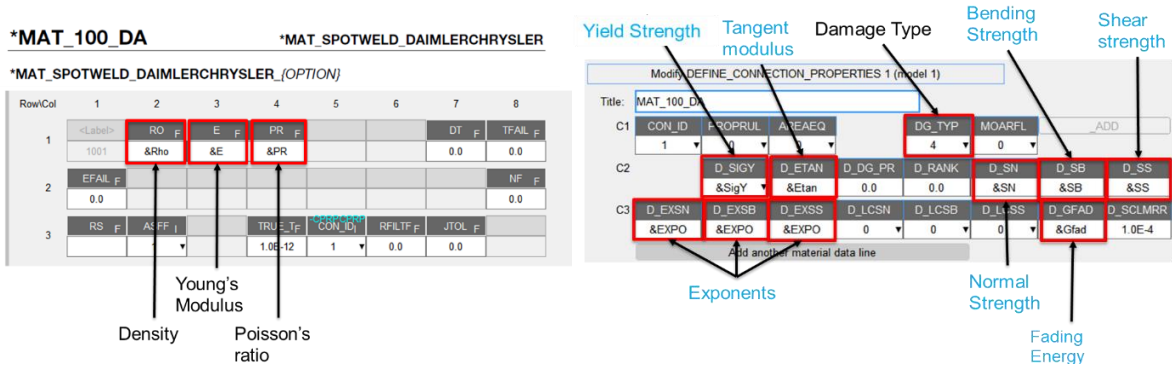


Fig.4: (a) *MAT_100_DA

(b) *DEFINE_CONNECTION_PROPERTIES

2.2 Post-Processing for *MAT_100_DA

Post failure was defined using multiple approaches which include strain-based damage, failure function-based damage and fading energy damage. (DGYPT = 1,2,3,4,5) [8].

Failure functions and individual failure terms were requested in DCFAIL file. SWFORC file was requested to plot spotweld forces and moments. (Refer to *DATABASE_ASCII). In addition to this, history variables were requested in d3plot and binout files. Table 2 shows list of history variables for *MAT_100_DA

History Variable #	
1	density
8	damage
10	effective strain rate
11	tensile strengths
12	shear strengths
13	bending strengths
18	failure function value
19	failure function normal term
20	failure function normal bending
21	failure function normal shear

Table 2: Solid History Variables for *MAT_100_DA model.

3 Physical Testing –

The following procedures were completed regarding material preparation, weld development, test specimen preparation, and specimen testing.

3.1 Introduction

The following procedures were completed regarding material preparation, weld development, test specimen preparation, specimen testing, and evaluation.

Coupons were cut to 150mm x 50mm on hydraulic shear with the rolling direction along the 150mm side. Configurations of the three types of tensile tests are in Fig.5, Fig.6, and Fig.7 and will be explained in further detail. The target nugget size for all material stacks was targeted based on industry standards and was governed by thinnest material layer. This was done to account for variance in the nugget sizes and to ensure a minimal number of welds have less than a target nugget diameter.

3.2 Weld Schedule Development

To confirm that the weld schedules met manufacturing standards, a robustness test was performed. Using freshly dressed electrodes, 36 welds were made and tested. During the spot-welding process, no expulsion or heavy sticking to the welding electrode was allowed. Then the weld surfaces on both sides were examined for expulsions, pinholes, or surface cracks at 20X magnification. If the

welds passed these checks, the first three and last three welds were cross-sectioned and checked for excessive porosity and cracking. The remaining 24 welds were peel tested. If more than 75% of the peeled welds had button-pull failures, the weld schedule was considered satisfactory.

3.3 Test Specimen Preparation

All tensile test coupons were welded using positioning fixtures to achieve the geometries as shown in Fig. 5, Fig.6, and Fig.7. Lap shear coupons, have 50mm x 50mm tabs welded to either side that allows the Instron to pull at the center plane of the test coupon as opposed to the coupon being mounted at a diagonal in the grips. Coach peel coupons were welded flat, then bent to a 6mm radius.

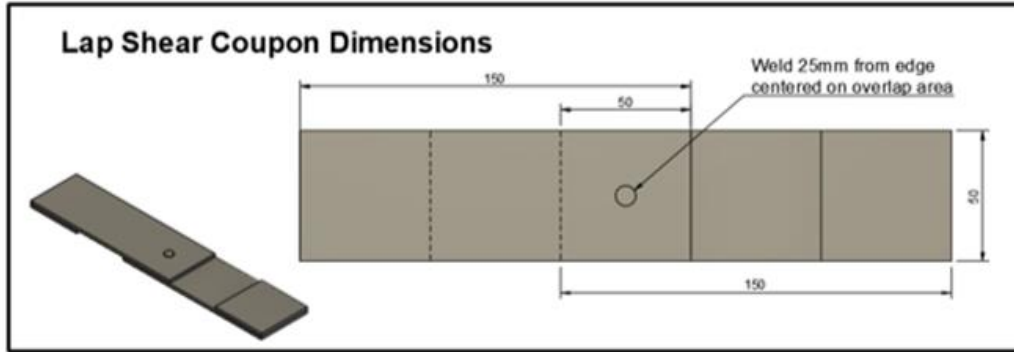


Fig.5: Lap Shear Coupon Dimensions

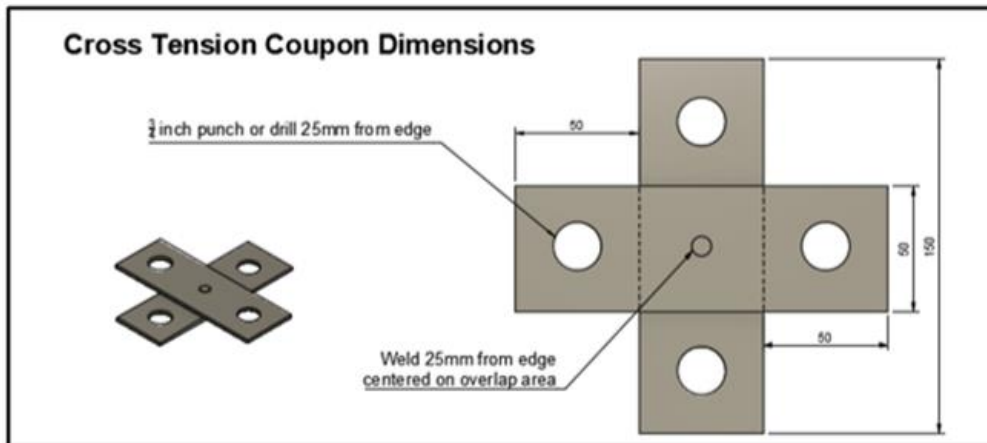


Fig.6: Cross Tension Coupon Dimensions

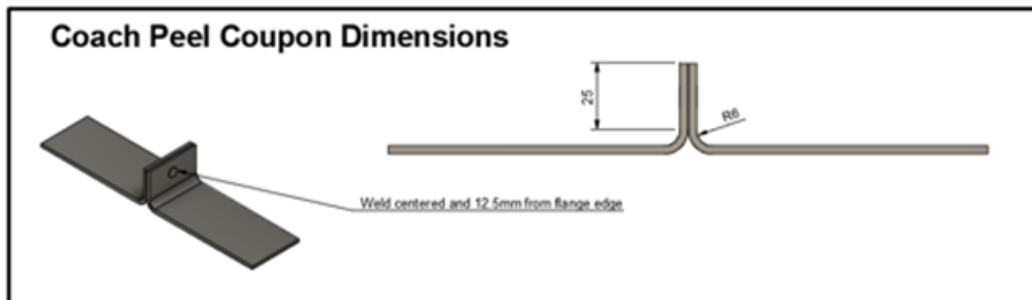


Fig.7: Coach Peel Coupon Dimensions

Electrodes degraded over time during the spot-welding process. The order of welding was staggered to make sure each type of test has increments of the degrading welding electrodes.

3.4 Specimen Testing

Before testing, positive and negative sides of the welding surface were examined at 20x magnification for any surface cracking, expulsions, or pinholes. All coupons were heat treated at 180°C for 20 minutes metal temperature with a maximum total time of 35 minutes in the oven, including a ramp-up time to simulate paint bake in a production line.

All testing was conducted on a tensile machine and pulled at 5mm/s with the use of digital extensometer gauges specific to each type of test. A digital extensometer gauge (highlighted in Fig.8 by yellow-colored arrows) was used for all samples to generate an extra set of displacement data. Extensometer data helped to capture accurate displacement (and hence energy absorbed) which improved CAE correlation. As shown in Fig.8, lap shear tests go into the grips with 50mm grip length, cross tension tests require a fixture to pull, and coach peel tests go into the grips with 50mm grip length.

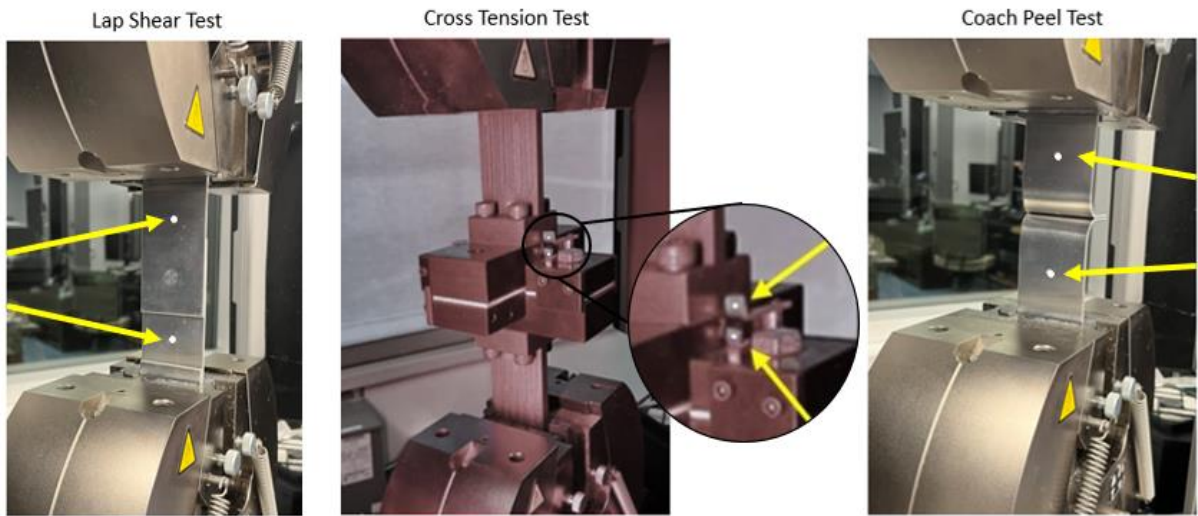


Fig.8: Lap Shear, Cross Tension, and Coach Peel Testing Set-up

After each sample was tested, the nugget size and failure mode were recorded. The Force-displacement data from tensile machine was used to correlate with CAE data. Examples of tested samples are shown in Fig. 9 below.

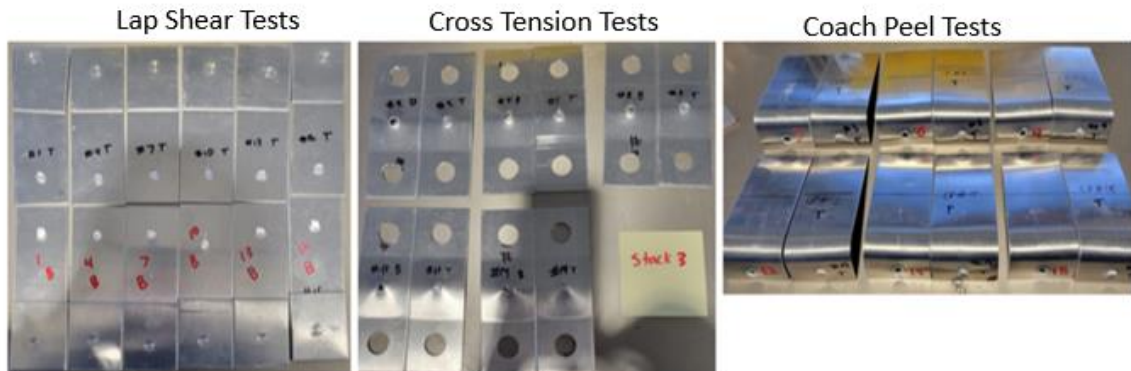


Fig.9: Lap Shear, Cross Tension, and Coach Peel Samples After Tensile Testing

KS-2 specimen testing was performed with U-shaped coupons consisting of 4 variations of testing as well as coach peel testing shown in Fig.10. The fixture depicted in Fig.11 was utilized for 0°, 30°, 60°, and 90° testing while the peel test coupons were clamped in the grips 25mm away from the center seam. KS-2 test data was later used to validate calibrated LS-DYNA failure cards.

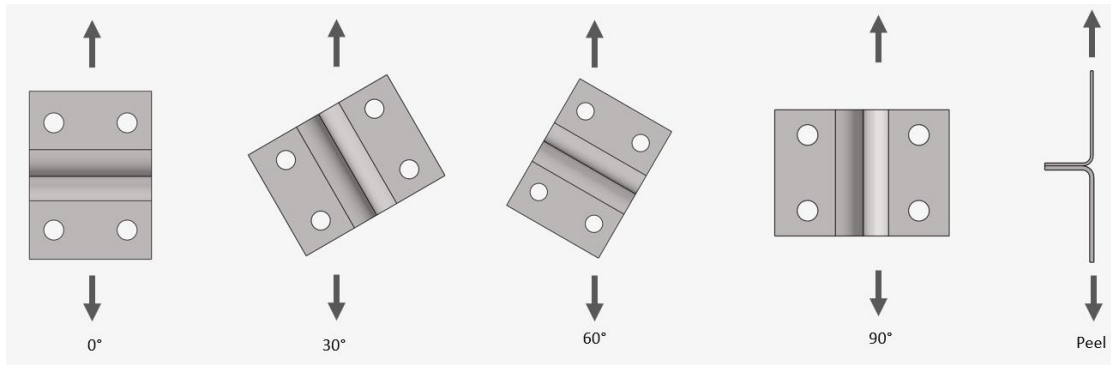


Fig.10: KS-2 Specimen Testing

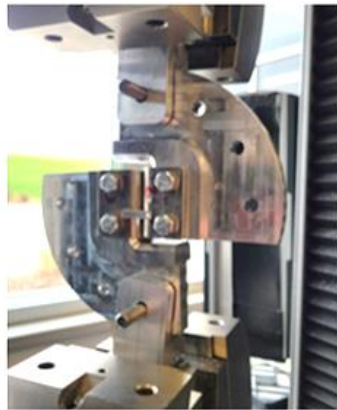


Fig.11: KS-2 0 Degree Set-up Example

4 Sensitivity Studies

4.1 Failure Parameters Sensitivity Study for *MAT_100_DA

A sensitivity study for failure parameters (SigY, Etan, SS, SN, SB, D_EX) during various loading conditions including combined loading cases was performed. For simplicity, the exponents D_EXSN, D_EXSB, D_EXSS were assumed to be the same value and labelled as D_EX. These parameter effects were plotted on a pareto plot (Fig.12 indicating their impact on the energy absorption for each load case.

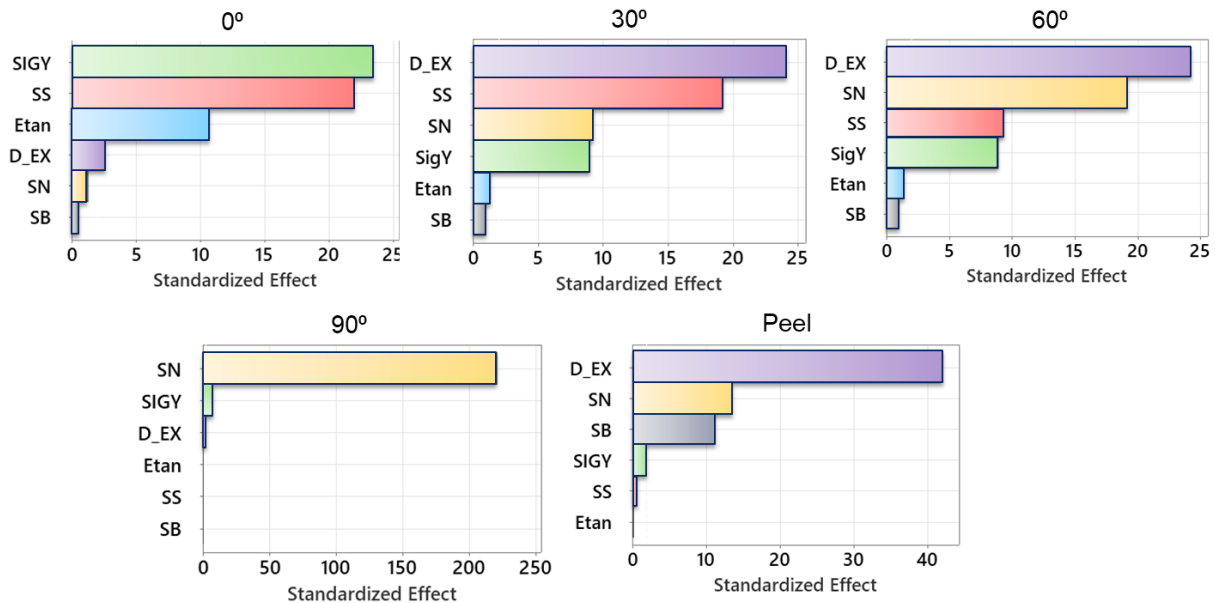


Fig.12: Pareto plot of energy vs main effects

During pure shear loading (Lap Shear 0°), SigY, Etan and SS are key parameters affecting the weld failure. During combined loading cases (KS-2 30° and 60°), the exponent (D_EX) had the highest impact

followed by SN and SS. For pure axial loading (Cross Tension - 90°), only the SN parameter had a considerable impact. For the bending case (Peel), the exponent had the highest impact followed by SN and SB.

This study gave valuable insights on sensitivity of failure parameters helped guide the development of the calibration process.

4.2 CAE Sensitivity Studies

4.2.1 Mesh size:

A mesh size sensitivity study was performed to find the effect of parent material mesh size on the weld failure. Element mesh sizes of 2mm, 3mm and 5mm were used for this study. Results of this study can be seen in Fig.13. It was observed that FEA prediction for the lap shear loading was not sensitive to mesh size, but it was dependent on mesh size in both axial and coach peel load cases.

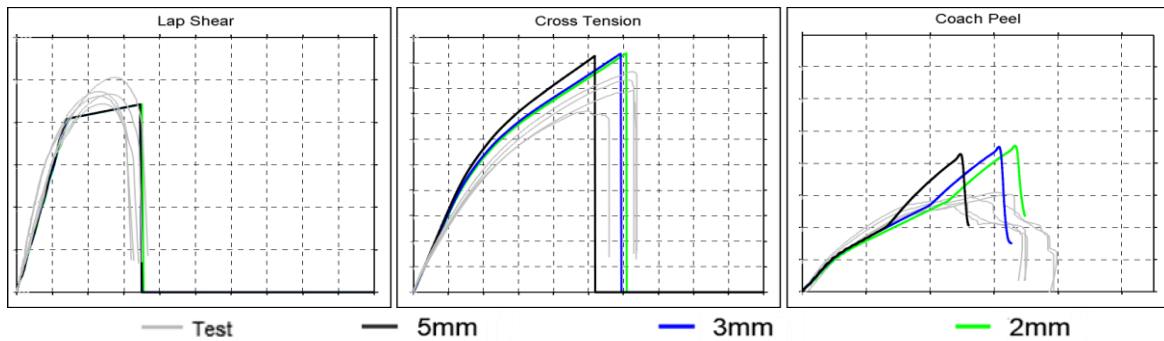


Fig.13: Force vs Displacement plot comparing different mesh sizes.

The reason for this sensitivity is that the larger element size fails to replicate local deformation and bending in the test coupon during axial and coach peel load cases. Smaller mesh size tends to represent more realistic behavior. Appropriate mesh size can be chosen based on desired accuracy and accordingly failure parameters should be tuned for each specific mesh size.

4.2.2 Weld Element Modeling Approaches:

3D Weld element can be represented by a single hex element or a hex cluster (through *DEFINE_SPOTWELD_ASSEMBLY). A sensitivity study was done to study differences in behaviors of a single hex element versus 4 and 8 hex clusters. 1D beam element was excluded since it is not supported by *MAT_100_DA material model. It was observed that (Fig.14) 1 hex shows early failure compared to 4 hex and 8 hex clusters in all load cases. In lap shear, it was observed that difference between 1 hex and hex clusters increases as value of ETAN (Hardening Modulus) reduces (Fig.15). The behavior of 1 Hex, 4 hex and 8 hex was very similar in cross tension test with minor differences in the displacement. Results from coach peel load case had a significant difference from 1 hex to 4 hex to 8 hex. Single hex element failed to realistically represent bending in the weld element and tied contact behavior (Fig.16) resulting in early failure. Hex clusters consist of multiple hex elements resulting in more accurate bending prediction and better tied contact behavior.

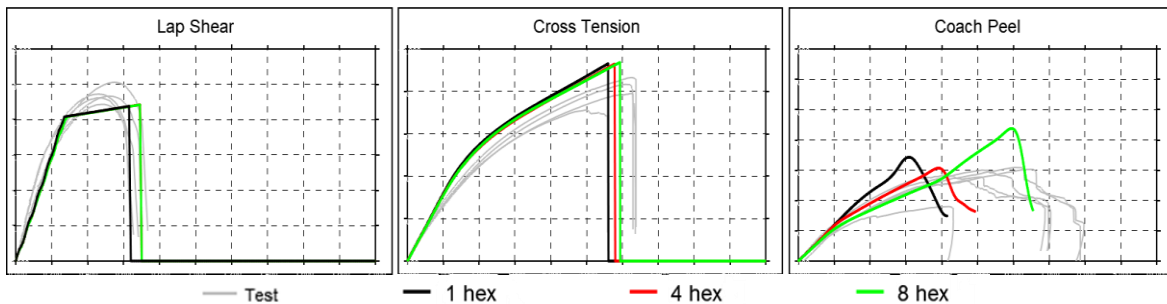


Fig.14: Force vs Displacement plot comparing different types of weld elements

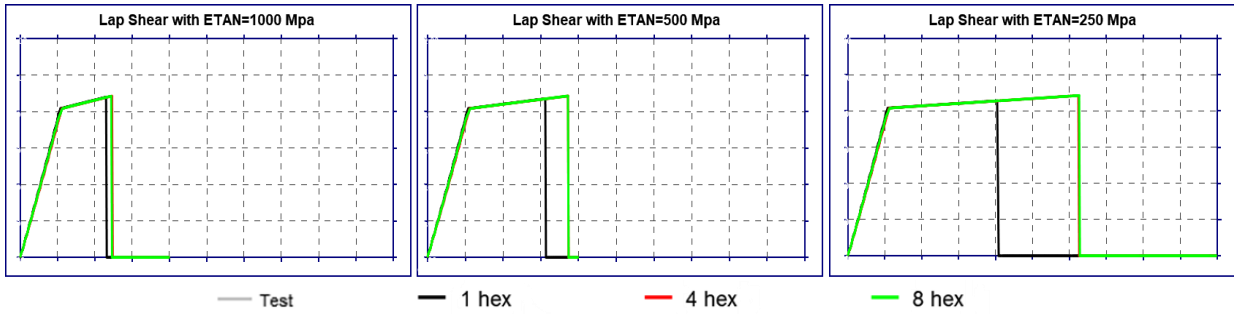
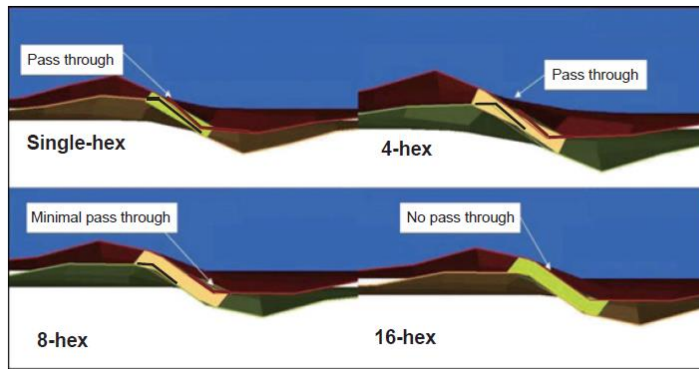


Fig.15: *Force vs Displacement plot Effect of ETAN on Weld Element Type*



Reference: *Improved Method to Assess Spot weld rupture in LS-DYNA using Solid Element Assemblies*, Skye Malcolm et al. April 2009 [8].

Fig.16: *Contact modelling of different type of weld elements*

4.2.3 Orientation of the Weld Element:

Weld creation by a pre-processor is typically automated when dealing with large scale models and it is hard to control orientation of weld element. Ideally, element orientation should not have any significant effect on failure behavior. However, it was observed that weld element orientation had considerable effect on the results depending upon type of weld element used. A sensitivity study of weld element orientation was conducted for 1 hex, 4 hex and 8 hex weld assemblies. The weld elements were oriented in various angles to the base mesh (See Fig.17) and the sensitivity due to the orientation of the elements were studied.

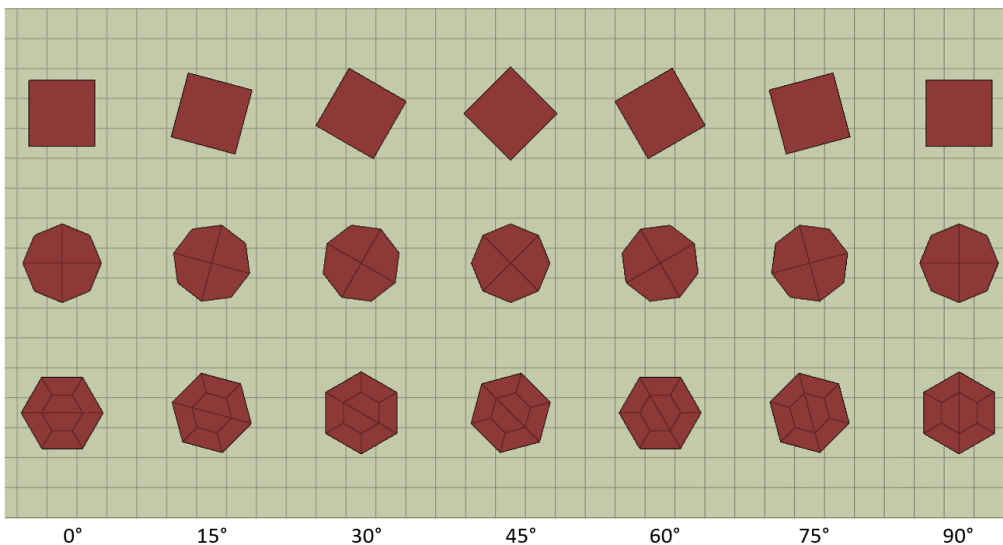


Fig.17: *Orientation of the weld elements at different angles to the base mesh.*

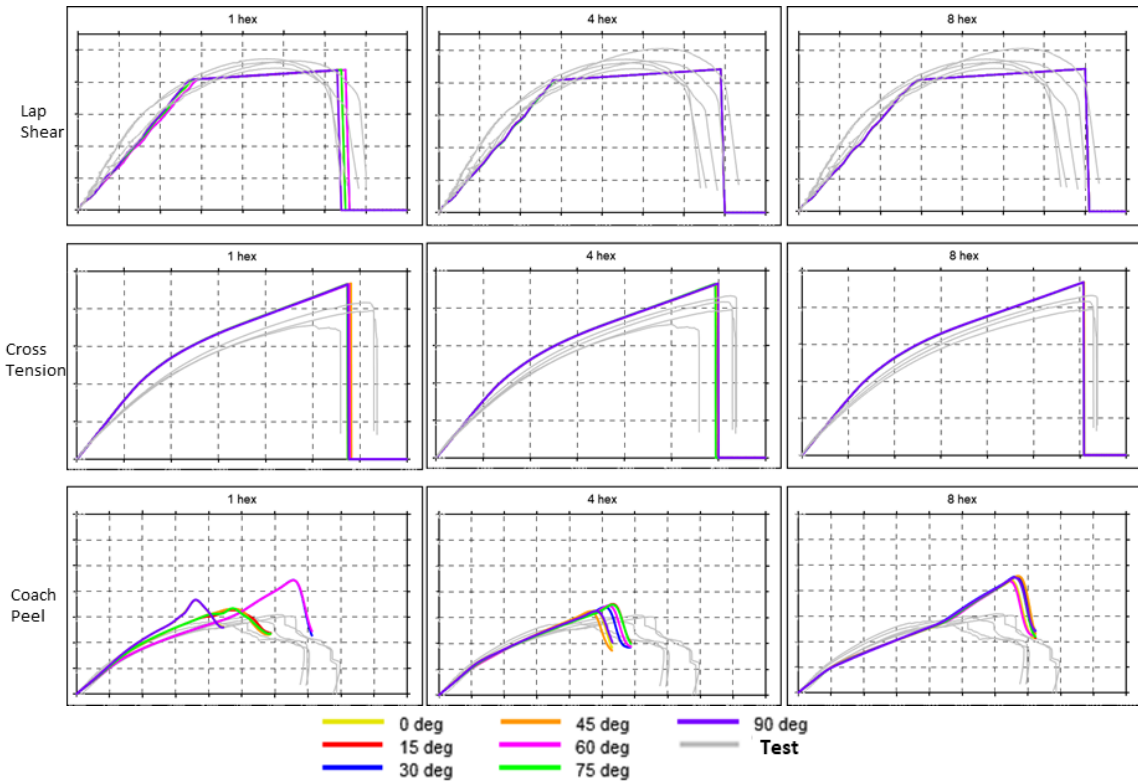


Fig.18: Force vs Displacement plot comparing different orientations of weld elements.

It was observed that (Refer Fig.18) lap shear and cross tension results showed negligible variation for various angles. The coach peel load case showed considerable variation in the load curve with various angles and weld element types. 1 Hex element is most sensitive to orientation whereas 8 hex is the least sensitive. 4 Hex element is in between 1 and 8 hex. Table 3 summarizes the findings from the sensitivity study with a comparison table.

	1 Hex	4 Hex	8 Hex
Sensitivity to element rotation	High	Medium	Low
Sensitivity to mesh size	High	Medium	Low
Bending behavior prediction	Poor	Fair	Good
Tied contact behavior	Poor	Fair	Accurate
Post Failure Damage Option	Behaves as expected	Issues when used with DGTYP 4 and 5 (refer section 5)	Issues when used with DGTYP 4 and 5 (refer section 5)
Overall accuracy	Fair	Average	High
Runtime in big scale models (with Mass Scaling)	Same	Same	Same

Table 3: Comparison Table for 1 Hex, 4 Hex, 8 Hex

5 Challenges while using damage for Hex Clusters

Two methods are implemented in `*MAT_100_DA` to improve the uniaxial loading behavior. More details can be found in LS-DYNA keyword manual [8].

- Method 1 – Young’s modulus as a negative number (old method)
- Method 2 – UNIAXIAL keyword extension (new method)

The first method sets the two transverse stress terms to zero with the goal of eliminating parasitic transverse stress that will prevent the damage function from growing as expected. This method can induce spurious oscillations in the axial force that leads to premature failure.

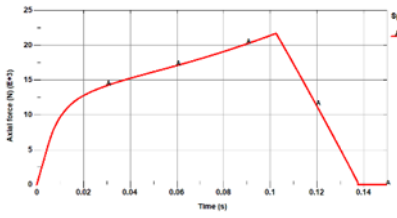
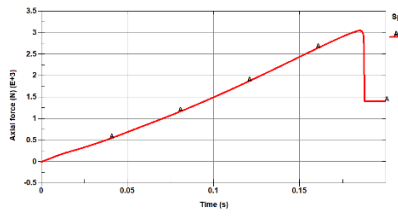
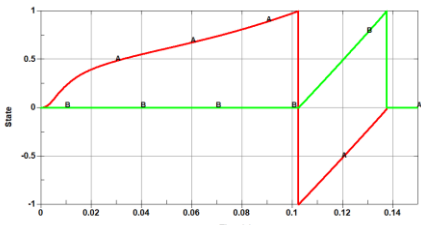
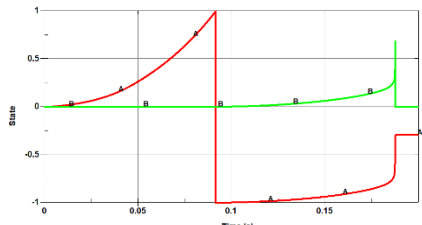
The second method, the UNIAXIAL option, sets the two transverse stress and strain terms to zero with the same goal as the first method, and to promote the smoothness of the damage function. The UNIAXIAL option is thus preferred.

During this study, it was early found that the damage function was not behaving as expected with a hex cluster for `DGTYP= 4` and `5`, even when using the UNIAXIAL option. However, the LS-DYNA Keyword Manual [8] and other available literature have not reported issues with the damage function for uniaxially loaded welded assemblies using a hex cluster. It appears that two welded plates with different stiffnesses i.e., with a different material and/or thickness, might also prevent the damage function to grow as expected, even when using the UNIAXIAL option since the local deformation in the plates generates relatively high shear stress components in the hex cluster. The hex cluster must be in a uniaxial stress state for the damage function to grow as expected. The behavior during damage thus depends on how fast the hex cluster will reach (or not reach at all) a uniaxial tension stress state.

Table 4 shows a case where the plates have the same stiffness and a case where plates do not. It can be observed that when the plates have different stiffnesses:

1. the spotweld force increases even after the failure initiation;
2. the damage slowly increases after the failure initiation;
3. stress components are not set to zero at the failure initiation;
4. failure is completed when the spotweld reaches a uniaxial state of stress.

It can be concluded that `DGTYP= 4&5` shows issues for hex clusters whereas `DGTYP=3` behaves as expected. All `DGTYP` options work as expected for 1 hex; however, 1 hex has other limitations as explained earlier.

	Case where plates have the same stiffness	Case where plates don't have the same stiffness
1	 <p>Expected force behavior</p>	 <p>Force increases even after the failure initiation</p>
2	 <p>Expected failure / damage behavior</p>	 <p>Damage slowly increases after initial failure</p>

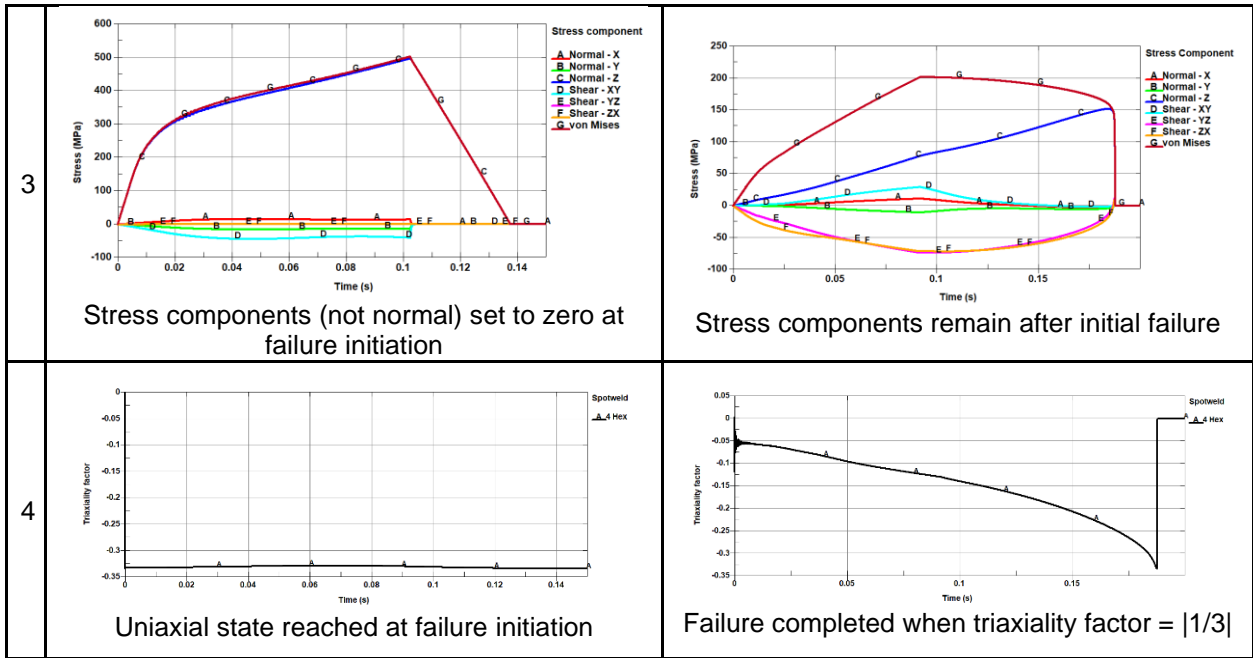


Table 4: Challenges in using DGTYP=4 and 5 while using hex clusters

DGTYP=3 works as expected and does not show these issues. However, DGTYP=3 has limitations in realistically describing damage behavior since fading energy calculation is based on simple strain-based approach using area of the triangle after failure initiation. While using hex clusters DGTYP=3 works better in the author's opinion.

$$\Delta \epsilon_{fading} = \frac{2 \times GFAD}{\sigma_{failure}} \tag{2}$$

GFAD is fading energy.

6 Card Calibration

While calibrating failure cards, the primary goal was to match total energy absorbed with the least deviation from the failure stress calculated from the tests. Sensitivity studies conducted on failure parameters (elaborated in section 3.1) were considered while calibrating the cards for each loading direction. Flat coupon test data (Lap Shear, Cross Tension and Coach Peel) were used to calibrate the cards while KS-2 test data were used for validation purposes.

The calibration process started with the lap shear loading where SS, Etan and SigY were calibrated. For cross tension test, SN value was calibrated. Finally, the SB value and exponents were calibrated using the coach peel model. Final values were fine-tuned through using an optimization routine. In optimization process, all failure parameters discussed earlier were considered as variables with the objective being to match total energy absorbed in the test. The minimum energy measured from the test samples was the objective function to ensure predicted failure energy results were conservative (e.g., predicted energy was less than actual energy measured on test). Fig.19 & Fig.20 show CAE-Test correlation examples of two stacks.

6xxx 3.0mm to 6xxx 3.0mm

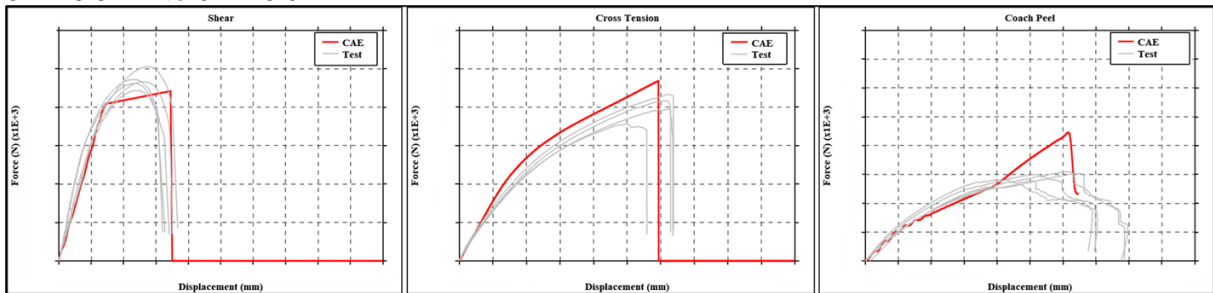


Fig.19: Force vs Displacement plot comparing the test to CAE results.

5xxx 1.1mm to 6xxx 3.0mm

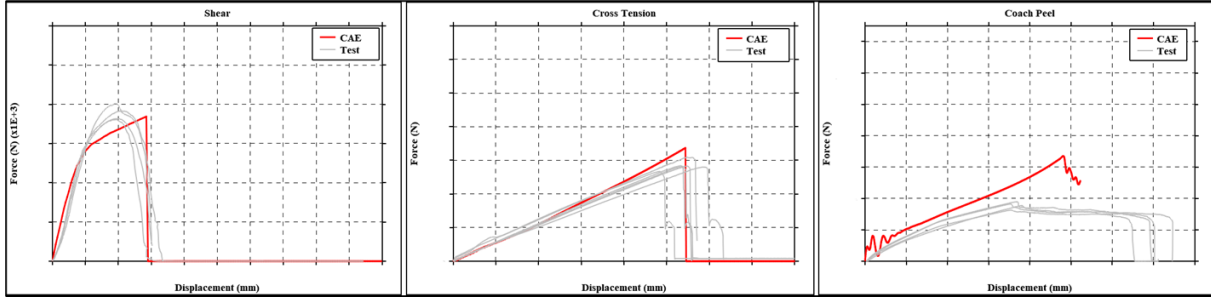


Fig.20: Force vs Displacement plot comparing the test to CAE results.

KS-2 Testing: KS-2 testing was conducted primarily to validate the calibrated cards for different loading angles (30°, 60°). Fig.21 shows correlation with KS-2 test data.

5xxx 1.1mm to 6xxx 3.0mm KS-2 Testing:

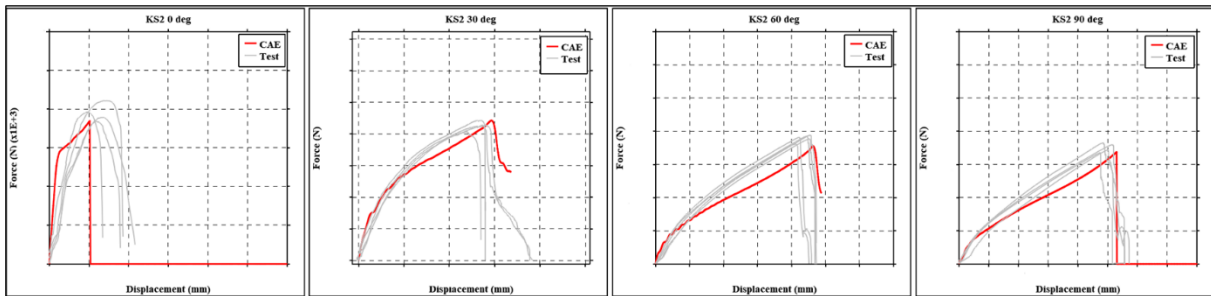


Fig.21: Force vs Displacement plot comparing the test to CAE results.

The KS-2 CAE model showed good correlation with the test data (less than 6% deviation) and weld failure cards were successfully validated.

7 Summary and Next Steps

In this work, spotweld modelling methodologies and failure characterization of aluminum RSW joints were studied. Out of many material models, ***MAT_100_DA** was chosen because of reduced reverse engineering effort and good accuracy in failure prediction. Reduced reverse engineering and staying closer to test data during the card calibration simplifies producing failure parameters for weld stacks through interpolation techniques or machine learning without doing additional physical testing.

Various CAE sensitivity studies provided valuable insights while defining modeling approach.

- 1 hex element is more sensitive to mesh size and element orientation. 8 hex have very consistent results.
- Smaller element sizes (2mm, 3mm) gave better results and failure prediction.
- It was found that care should be taken while using damage (DGTYP=4 and 5) for hex assemblies under axial loading.
- DGTYP=3 behaves normally but has its limitations in realistically predicting damage.

Overall, failure cards calibrated using this process gave good correlation (less than 6% deviation from test energy on average) with the test data and minimal reverse engineering effort. This approach will help in generating a larger database of failure parameters and potentially allow failure parameter prediction for weld stacks without physical testing through machine learning. A similar exercise is planned to be conducted on self-piercing rivets in the near future.

8 Literature

- [1] Andrew Halonen, Mayflower Consulting LLC., "Alumobility Introduces a New Generation of Aluminum Doors." Light Metal Age, August 2021.
- [2] Luo, Alan. (2021). "Recent advances in light metals and manufacturing for automotive applications." CIM Journal. 12. 1-9., doi:10.1080/19236026.2021.1947088.
- [3] DuckerFrontier. (2020). 2020 North America light vehicle aluminum content and outlook (July 2020). Washington DC, USA: DuckerFrontier.
- [4] Koralla, S., Gadekar, G., Nadella, V., and Dey, S., "Spot Weld Failure Prediction in Safety Simulations Using MAT-240 Material Model in LS-DYNA," SAE Technical Paper 2015-26-0165, 2015, doi:10.4271/2015-26-0165.
- [5] Zhang, F., Xu, H., & Fang, X. (2020). Failure behavior and crash modelling of resistance rivet spot welding (RRSW) for joining Al and steel in vehicle structure. International Journal of Crashworthiness, 27(1), 243–260. <https://doi.org/10.1080/13588265.2020.1786269>
- [6] Sike Sommer and Johannes Maier., "Failure Modeling of a Self-Piercing Riveted Joint using LS-Dyna.", presented at 8th European LS-Dyna Conference, 2011.
- [7] Seeger, F.D., Feucht, M., Keding, B., & Haufe, A.D. (2005). An Investigation on Spot Weld Modelling for Crash Simulation with LS-DYNA. (2005).
- [8] LS-DYNA Keyword User's Manual Volume 1 and 2, Version R13, Livermore Software Technology Corporation (LSTC), Livemore (USA), 2021.
- [9] Malcolm, Skye. "Spotweld Failure Prediction in LS-Dyna using Solid Element Assemblies." (2007).